# Theoretical phase diagram of beryllium at low pressure and high temperature

Gregory Robert, Philippe Legrand, and Stephane Bernard

Citation: AIP Conference Proceedings **1426**, 1203 (2012);
View online: https://doi.org/10.1063/1.3686496
View Table of Contents: http://aip.scitation.org/toc/apc/1426/1
Published by the American Institute of Physics

# THEORETICAL PHASE DIAGRAM OF BERYLLIUM AT LOW PRESSURE AND HIGH TEMPERATURE

**G. Robert, P. Legrand and S. Bernard**

*CEA, DAM, DIF, F-91297 Arpajon, France*

**Abstract.** We will try to shed some light on a controversial issue on the phase diagram of beryllium: the very existence of the bcc structure at low pressure and high temperature. In the density functional theory plus quasi-harmonic modeling framework (DFT-QHA), we show that the bcc phase can be dynamically stable at low pressure in a small region delimited by the ρ=2100 kg/m$^3$ isochore only if large anharmonic effects i) overcome the imaginary $N$-$T_1$ mode obtained at T=0 K in the phonon spectrum ii) lead to sufficient amount of entropy to promote the free energy of the bcc phase. Force and velocity averages and melting curves obtained by quantum molecular dynamics (QMD) with 54 atoms in the cell indicate that only the former condition is fulfilled.

**Keywords:** Beryllium, Density functional theory, Molecular dynamics.
**PACS:** 64.30.Ef, 31.15.A-, 62.20.de.

## INTRODUCTION

Beryllium, although a "simple" metal remains a challenge for both theory and experiment. In the sole experimental phase diagram under pressure (up to 6 GPa) of François *et al.* [1], a bcc structure at high temperature appears below the melting curve. Despite many successes to predict numerous properties of beryllium, DFT-QHA is unable to predict the stability of the bcc structure in this domain [2][3]. At 0 K, a phonon imaginary frequency $N$-$T_1$ mode appears in the bcc phonon spectrum for densities lower than 2100 kg/m$^3$. To go beyond, we have to evaluate the anharmonic effects which can be able to stabilize the $\Gamma$-$N$-$T_1$ branch in temperature and bring enough entropy to lower the free energy of the bcc below the hcp one.

After a brief review of experimental data and QHA-DFT results on elastic constants and phase diagram, we use quantum molecular dynamics to show the weak influence of anharmonicity on hcp and high pressure bcc phases and its major role on the hypothetical low pressure bcc phase.

## EXPERIMENTAL REVIEW AND DFT-QHA RESULTS

In 1959, Martin *et al.* [4] observed two thermal arrests of the electrical conductivity in the melting region (1542 and 1556 K). Using X-ray analysis, the first arrest was attributed to a hcp to bcc phase transition, and the second to melting. However, they advanced the hypothesis that "*hcp-bcc is not observed in pure beryllium"*. In 1965, François *et al.* [1] proposed a rough sketch of the phase diagram. Their work, based on electrical conductivity measurements, seems to exhibit also two thermal arrests. However, François *et al.* underline the importance of reactivity of beryllium and the insufficient purity of their samples (recrystallization phenomena from impurity in samples or from transmitting media). On the other hand, recent DAC measurements with X-ray

*Shock Compression of Condensed Matter - 2011*
AIP Conf. Proc. 1426, 1203-1206 (2012); doi: 10.1063/1.3686496

analysis show no evidence of a bcc phase domain. [5]. Thus, revisiting old data on beryllium seems to be necessary.

To do this, DFT-QHA is a perfect tool: all recent experimental data on hcp are well reproduced (isotherms, phonons…). For example, the Helmholtz free energy function of density ρ, temperature T and strain $\varepsilon_{ij}$ can be defined. Then, using the strain-energy equation of Barron and Klein, isothermal elastic constants $c_{ij}(\rho,T)$ are determined. Applying our DFT-QHA EOS, theoretical isothermal $c_{ij}(p,T)$ are obtained and compared to experimental adiabatic $c_{ij}(p,T)$ (Table I and Figure 1).

**TABLE 1.** Theoretical and experimental elastic constants pressure derivatives.

| | **This work** | **Exp[6]** |
|---|---|---|
| $dc_{11}/dp$ | **6.0±1** | **6.92(3)** |
| $dc_{33}/dp$ | **7.6±1** | **8.98(3)** |
| $dc_{44}/dp$ | **2.2±1** | **2.55(3)** |
| $dc_{12}/dp$ | **1.7±1** | **2.76(3)** |
| $dc_{13}/dp$ | **0.6±1** | **3.3(1)** |

Concerning the sole experimental measurements $c_{ij}(T)$ which exist above 300 K [7] they must be compared to the recent longitudinal and transversal sound velocities measurements [8]. Using Voigt-Reuss-Hill average, polycrystalline bulk modulus is deduced and compared to experiments.

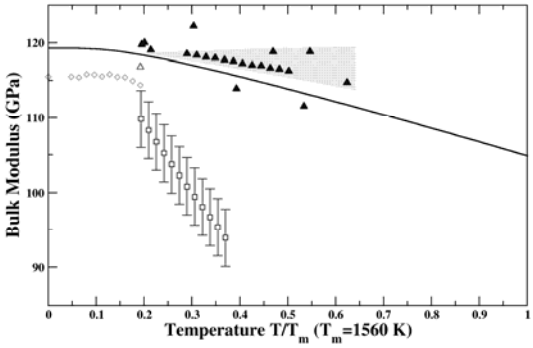


**Figure 1.** Adiabatic bulk modulus along 1 bar isobar from our EOS (full line). Diamonds [7], square [9], empty triangle up [10] and full triangle up [8] reproduce experimental VRH adiabatic modulus.

DFT-QHA is able to reproduce recent experimental sound measurements as well as data available below T=300 K, except for Rowland *et al.* measurements [7]. Thus, the latter seem to be doubtful.

Now, we will turn to phase diagram predicted by DFT-QHA: among the 5 structures studied (hcp, bcc fcc, α-Sm and α-U) only an hcp phase and a bcc under high pressure appear in the DFT-QHA phase diagram (Figure 2).

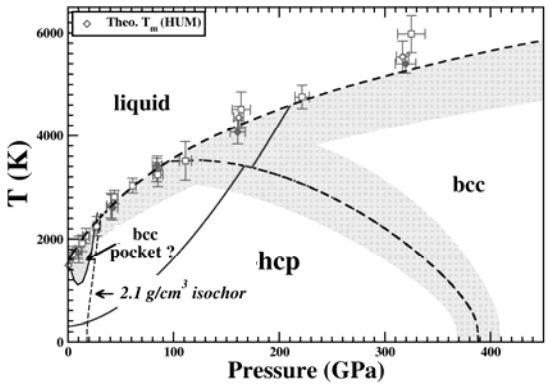


**Figure 2.** Phase diagram predicts by DFT-QHA (dashed lines). Symbols reproduced melting temperature obtained by Heat-Until-Melt method. Gray parts are the uncertainties estimate in the calculations. Full line is the main Hugoniot Curve.

The imaginary frequency at $N$-$T_1$ high symmetry point in the bcc structure below 2100 kg/m$^3$, prevents it to be stable. Therefore, to exist in this domain, anharmonic effects, missing in DFT-QHA results, have to prevail.

The aim of the next part is to check the influence of anharmonic terms.

## QMD CALCULATIONS

### Anharmonic effects in hcp and high pressure bcc phases

A way to estimate anharmonicity is to compare the pressure-temperature along Hugoniot/isentrope obtained by DFT-QHA and those obtained through direct QMD calculations [11].

Numerical procedure is as follow [12]:
two structures (hcp and bcc) are thermalized during 20 ps at the reference state ($\rho_0$=1841.4 kg/m$^3$, T=300 K) using Nosé-Hoover thermostat. The plane wave cut-off is 350 eV. The **k**-points sampling is 14 for the hcp and 4 for the bcc. The

c/a ratio for hcp is supposed to be independent of temperature [2]. Consequently, we retained the c/a(V) obtained in QMD calculations at 0 K. Once the system is thermalized, it is isotropically compressed to the desired density; then the temperature is slowly increased (0.1 to 0.5 K /ps) by increasing kinetic energy.

We define $D_{RH}$ as the departure from the Rankine-Hugoniot solution (Figure 3):

$$D_{RH}=[(e-e_0)- \tfrac{1}{2}[(p+p_0)(1/\rho_0-1/\rho)]], \quad (1)$$

Temperature $T_V$ along an isentrope is determined from a previous step labelled 0:

$$T_V=T_{V0}exp[-\Delta P/(k_B\Delta T)|_0(V-V_0)], \quad (2)$$

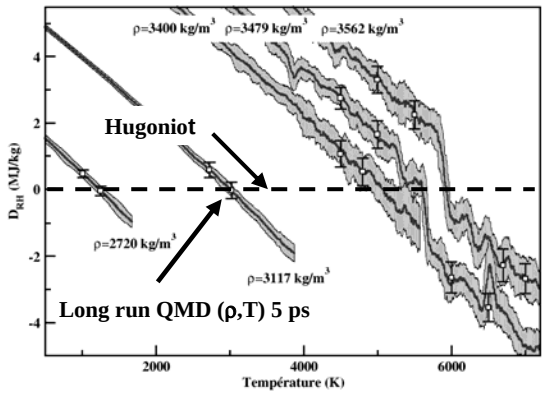


**Figure 3.** Departure from the Rankine-Hugoniot solution obtained by QMD function of density and temperature. Gray area is the fluctuation in the calculations; black area is an average. Symbols are long run QMD of 5 ps and a cell containing 128 atoms.

This method is numerically very efficient and relatively accurate to directly tabulate, from DFT, a whole phase.

The main disadvantage is that the phase transitions are ill determined: the solid–liquid temperature transition is not controlled (depends on the simulation box of course but also of the temperature ramp) and solid-solid transition could be missed. Then, the phase diagram must be known separately. Using the DFT-QHA phase diagram, shock-melting should take place around 200 GPa and T~4000K with a plateau width Δp of 30 GPa (Figure 4).

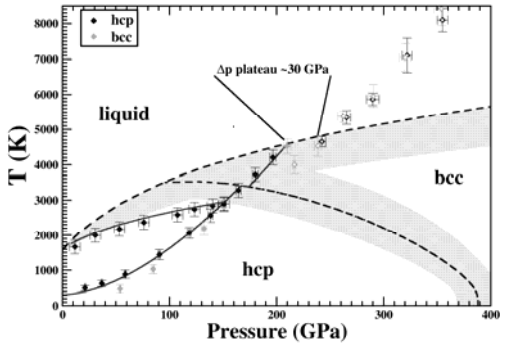


**Figure 4.** Main Hugoniot and an isentope obtained by DFT-QHA (solid line) and by QMD (symbols). Gray symbols use bcc has starting structure, black hcp. Full symbols are for solid and empty symbols for liquid.

The difference between DFT-QHA and direct QMD is rather small and confirms that anharmonic effects are weak. This is in agreement with the QMD calculations of Benedict *et al.* who use another QMD diagnostic for anharmonicity [13].

## Anharmonic effects in low pressure bcc phase

To estimate anharmonic effects at low pressure, we undertake QMD calculations in the supposed bcc pocket area (Figure 5). Two cells (hcp and bcc) which contain 54 atoms are constructed and thermalized during 20 ps using Nosé-Hoover thermostat. The **k**-points sampling is unchanged.

The first thing to note is that bcc cell melts before hcp one. This can indicate that bcc has the highest free energy. However, the small cell size can affect this observation.

The second thing to note is that if experimental equilibrium densities of hcp ($\rho_0$=1710 kg/m$^3$) and liquid ($\rho_0$=1600 kg/m$^3$) are coherent with QMD results (1730 kg/m$^3$ and 1620 kg/m$^3$ respectively), QMD fails to reproduce hypothetical experimental equilibrium density of bcc (1780 kg/m$^3$ from experiment and 1720 kg/m$^3$ from QMD). This means that the difference between hcp and bcc which is 60 kg/m$^3$ from experimental data is almost inexistent in QMD.

Thus, according to Clausius-Clapeyron relation, the temperature transition $T_T$ should be independent of the pressure and the hcp-bcc line transition should be a straight line.

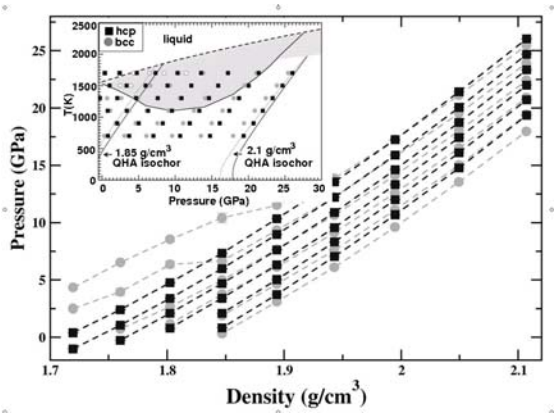


**Figure 5.** Isotherms obtained by QMD calculations in the supposed bcc pocket area. Gray symbols use bcc has starting structure, black hcp.

Moreover, pΔV term does not contribute in free energy difference between solid phases. Thus, to offset the 0 K energy difference ($\Delta E/k_B$=880 K) at $T_T$=1500K, only entropy plays a role and the bcc Debye temperature $\theta_D$(bcc) must be 20 % lower than hcp one ($\ln[\theta_D(\text{hcp})/\theta_D(\text{bcc})] \approx \Delta E/[3k_B.T_T]$).

Expressing forces $\mathbf{f}_i$ and velocities $\mathbf{v}_i$ obtained during QMD run in term of Debye temperature:

$$\theta_D \propto [\langle \mathbf{f}_i \rangle / \langle \mathbf{v}_i \rangle]^{1/2}, \quad (3)$$

we remark that $\theta_D$(hcp) and $\theta_D$(bcc) are close and mainly unchanged between QMD and DFT-QHA calculations for the hcp phase. Consequently, the 0 K energy difference is weakly affected by the temperature.

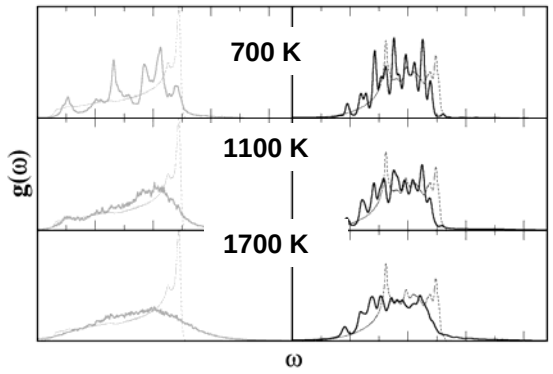


**Figure 6.** Phonon spectrum obtained from QMD (full lines) for bcc (left captions) and hcp (right captions) at ρ=1850 kg/m$^3$. Dashed lines reproduced real part of the DFT-QHA phonons spectrum. At 1700 K, the left caption reproduce the phonons spectra of a liquid.

Now, if we use Fourier transform of the velocity correlation $\gamma(t)=\langle \sum \mathbf{v}_i(t).\mathbf{v}_i(0) \rangle / \langle \sum \mathbf{v}_i(0)^2 \rangle$, to extract phonon spectra, we observe that the bcc phonon spectrum is more temperature sensitive than the hcp one (Figure 6). The rugged phonon spectrum of the bcc at T= 700 K becomes smooth at T= 1100 K. This seems to indicate a significant reorganization of the frequencies which can indicate a dynamic stabilization of this phase.

## CONCLUSIONS

Force and velocity averages and melting curves suggest that bcc is dynamically stable but its free energy is higher than hcp one. However, to be more quantitative, a significant work from QMD is needed: larger cells (at least 250 atoms), determination of the temperature for which the *N-T1* frequency becomes real or direct calculation of the free energy by thermodynamic integration for the 3 phases.

Moreover, as cast beryllium is extremely sensitive to impurities/environment at high temperature, such effects may be considered.

## REFERENCES


1. François, M. and Contre, M. in Proc. Grenoble 1965, PUF Paris (1966).
2. Robert G., Legrand P., Bernard S., Phys Rev B **82**, 104118 (2010).
3. Benedict L. X. *et al.* Phys Rev B **79**, 064106 (2009).
4. Martin A. J. and Moore A., J. Less-Common Met. **1**, 85 (1959).
5. Evans *et al.* cited in [3].
6. Silversmith D.J. *et al.*, Phys Rev B **1**, 567 (1970).
7. Rowland *et al.*, J. Phys F: Met. Phys. **2**, 231 (1972).
8. Nadal *et al.* J. Appl. Phys. **108,** 033512 (2010).
9. Migliori *et al.*, J. Appl. Phys, **95**, 2436 (2004).
10. Smith J.F. *et al.* J. Appl. Phys, **31**, 99 (1960)..
11. Kresse G. and Joubert D. Phys Rev B **59**,1758 (1999).
12. Matsson A. E. *et al.*, 14th International Symposium, Cœur d'Alène (2010)
13. Benedict L. X. *et al.* APS March Meeting (2008).